Cancer Cell, Volume *29*

Supplemental Information

miR-126 Regulates Distinct Self-Renewal Outcomes in Normal and Malignant Hematopoietic Stem Cells

Eric R. Lechman, Bernhard Gentner, Stanley W.K. Ng, Erwin M. Schoof, Peter van Galen, James A. Kennedy, Silvia Nucera, Fabio Ciceri, Kerstin B. Kaufmann, Naoya Takayama, Stephanie M. Dobson, Aaron Trotman-Grant, Gabriela Krivdova, Janneke Elzinga, Amanda Mitchell, Björn Nilsson, Karin G. Hermans, Kolja Eppert, Rene Marke, Ruth Isserlin, Veronique Voisin, Gary D. Bader, Peter W. Zandstra, Todd R. Golub, Benjamin L. Ebert, Jun Lu, Mark Minden, Jean C.Y. Wang, Luigi Naldini, and John E. Dick

SUPPLEMENTAL DATA

A

AML	Relapse or Diagnosis	FAB	Age	Sex	Karyotype	Engraftment of AML Subpopulations			
						$CD34^+$ $CD38^-$	$CD34^+$ $CD38^-$	$CD34^-$ $CD38^+$	$CD34^-$ $CD38^-$
1	Relapse	M2	48	F	46, t(2;21)(p21;q22)[4]/46,9(1;21)(q22;q22)	+	+	-	-
2	Diag	M5a	58	F	46, XX	+	+	-	-
3	Diag	unclass	52	F	47, XX, +8	+	+	+	+
4	Diag	unclass	62	M	46, XY	+	+	-	+
5	Diag	M5a	39	F	47, XX,+8	+	+	-	-
6	Diag	unclass	80	F	46, XX	+	+	-	-
7	Diag	M5	48	M	no data	+	NT	NT	+
8	Diag	M1	72	F	46, XX	+	-	-	-
9	Diag	M2	47	F	46,t(2:21)[4]/t(6:21)[2]/t(15:21)[2]	+	NT	NT	NT
10	Diag	M2	62	F	47,XX, +13	+	NT	NT	NT
11	Diag	M1	45	F	46, XX	+	+	-	-
12	Diag	M4eo	39	M	46,inv(16)(p13;q22)	+	-	NT	-
13	Diag	M5a	75	M	46, XX	-	-	-	-
14	Diag	M4	23	M	46, XY	NT	-	-	-
15	Diag	M5a	40	M	46, XY	+	+	-	-
16	Diag	M5b	80	M	no data	NT	-	-	-

B

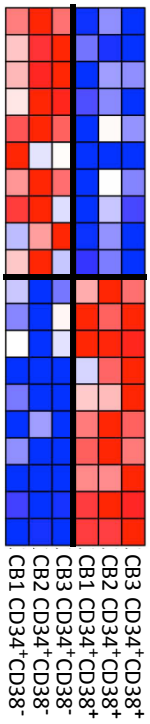

Probe	q value
hsa-miR-10a	0.34
hsa-miR-23b	0.39
hsa-miR-125a-5p	0.51
hsa-miR-342-3p	0.58
hsa-miR-10b hairpin	0.60
hsa-miR-326	0.60
hsa-miR-92b	0.74
hsa-miR-10b	0.76
hsa-miR-92a	0.76
hsa-miR-23a	0.76
hsa-miR-15b	0.59
hsa-miR-let-7d	0.58
hsa-miR-20b	0.58
hsa-miR-128	0.58
hsa-miR-98	0.58
hsa-miR-130b	0.34
hsa-miR-766	0.34
hsa-miR-486-5p	0.13
hsa-miR-20a	0.01
hsa-miR-181c	0.01

C

Population	Probe	q value
$CD34^+/CD38^-$		
	hsa-mmu-let-7b	0.0000
	hsa-mmu-let-7f	0.0138
	hsa-mmu-let-7a	0.0155
	hsa-mmu-miR-326	0.0371
$CD34^+$		
	hsa-mmu-let-7b	0.0000
	hsa-mmu-let-7a	0.0049
	hsa-mmu-let-7c	0.0089
	hsa-mmu-let-7f	0.0181
	hsa-miR-486-5p	0.0854
	hsa-mmu-miR-451	0.0854
	hsa-mmu-542-3p	0.0089
	hsa-miR-299-5p	0.0087
	hsa-mmu-miR-363	0.0013

Population	Probe	q value
BULK		
	hsa-mmu-let-7b	0.0000
	hsa-mmu-miR-425	0.0009
	hsa-mmu-let-7a	0.0061
	hsa-mmu-let-7c	0.0579
	hsa-mmu-miR-221	0.0579
	hsa-miR-520a-5p	0.0986
	hsa-miR-329	0.0885
	hsa-miR-193a-3p	0.0579
	hsa-miR-598	0.0566
	hsa-miR-525-3p	0.0490
	hsa-mmu-miR-26a	0.0325
	hsa-mmu-miR-542-3p	0.0064
	hsa-mmu-miR-186	0.0036
	hsa-miR-202	0.0026
	hsa-miR-299-5p	0.0013
	hsa-mmu-miR-363	0.0006

Figure S1, related to Figure 1. Generation an HSC-enriched miRNA signature and bioinformatic comparison of miRNA enriched in AML and CB fractions.

(A) Table detailing the clinical attributes of 16 AML patient samples used for the generation of a miRNA enriched LSC signature. A (+) denotes a sorted AML fraction the contained leukemia-initiating capacity in vivo, while (-) signifies no such activity was present after transplantation. (NT) indicates fractions that were not tested.

(B) Heat map depicting the top 10 miRNA candidates enriched within the human $CD34^{+}CD38^{-}$ HSC compartment and those enriched within the $CD34^{+}CD38^{+}$ committed hematopoietic progenitor population.

(C) Table of statistically significant miRNA probes enriched in AML (red type) or human lin^{-} CB (blue type) after informatic comparison of normal CB and malignant $CD34^{+}CD38^{-}$, $CD34^{+}$ or bulk cellular populations.

Table S1, related to Figure 1. Clinical and Molecular Characteristics of Patients Analyzed via Nanostring (PMCC Cohort)

	n=74
Male sex [n (%)]	36 (49%)
Age at AML diagnosis [years]	
median (range)	51.4 (23.2-75.9)
WBC count at diagnosis ($x10^9$/L)	
median (range)	18.2 (0.3-207)
% Blasts in PB at diagnosis	
median (range)	57 (0-98)
% Blasts in BM at diagnosis	
median (range)	70 (20-96)
Sample Material	
Bone Marrow [n (%)]	57 (77%)
Peripheral Blood [n (%)]	17 (23%)
Molecular Data [n (%)]	
mutated NPM1 (n=67)	36 (54%)
FLT3-ITD (n=67)	0
Treatment Approach	
Induction	74 (100%)
Allogeneic Transplant	19 (26%)
in CR1	7 (37%)
in CR2	12 (63%)

All samples were from diagnosis and had normal cytogenetics

A

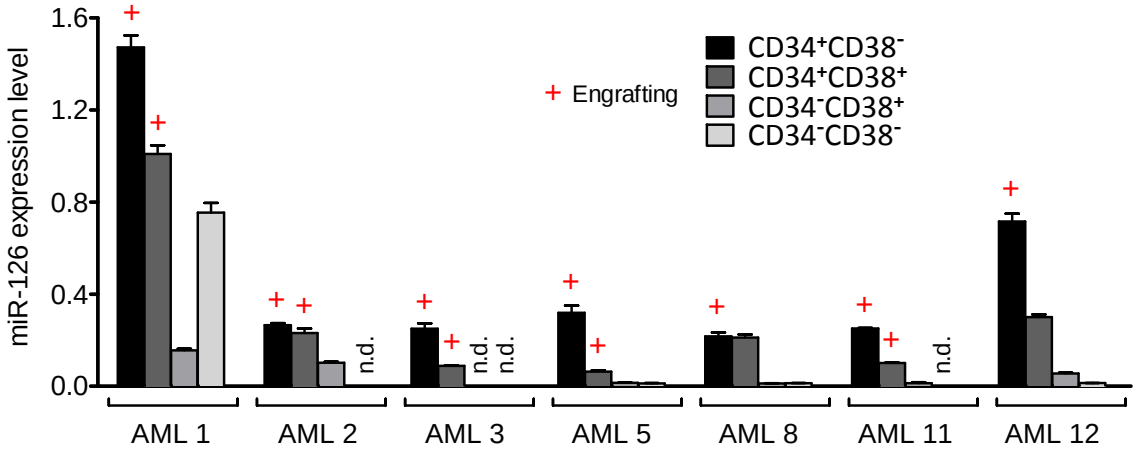

B

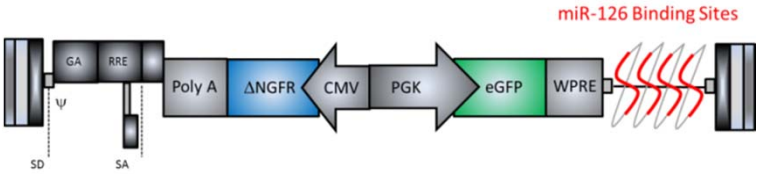

C

AML Sample	Population Gate	Fold miR-126 Enrichment from bulk	Fold miR-126 Enrichment from eGFP^{high}
AML 3	G6	0.08	1
	G5	3.2	43.1
	G4/G3	0.28	3.7
AML 7	G6	0.08	1
	G5	0.27	3.39
	G4/G3	3.39	42.3
AML 18	G6	0.02	1
	G5	1.16	45.4
	G4/G3	0.35	16

D

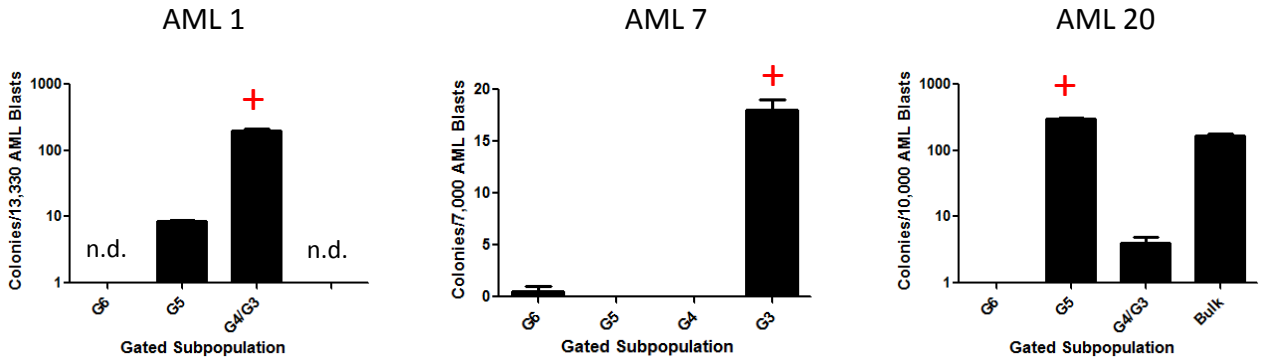

E

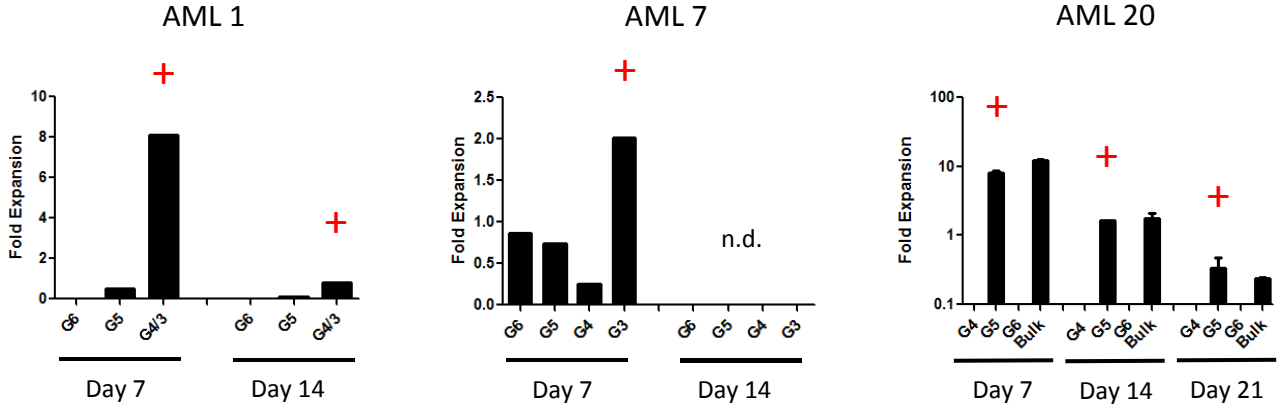

Figure S2, related to Figure 2. AML leukemia initiating capacity co-segregates with proliferation and clonogenic capacity of AML blasts.

(A) Quantitative PCR (qPCR) for mature miR-126 levels in flow sorted AML sub-fractions (see scheme depicted in **Figure 1A**). Data was normalized to RNU48 control levels. Results are shown as mean ± SEM of n=3 technical replicates.

(B) Schematic of the bi-directional miR-126 biosensor vector. The vector expresses truncated NGFR in one direction (which marks all transduced cells) and eGFP in the other direction. miR-126 binding sites are cloned downstream of eGFP. The more miR-126 a cell expresses, the less eGFP protein that is translated, leading to lower levels of eGFP fluorescence.

(C) Table depicting the normalized levels of mature miR-126-3p in biosensor sorted AML populations and measured by qPCR. In red text, the table shows the gated population most enriched in miR-126-3p levels compared to bulk AML or compared to $eGFP^{high}$ fractions (lowest miR-126 activity).

(D) Bar graphs representing the colony forming ability of flow sorted populations of miR-126 biosensor vector transduced primary AML patient samples after recovery from NSG mice. The red crosses indicate the gated populations that were able to recapitulate the AML ΔNGFR/eGFP hierarchy in vivo. Data represents mean ± SEM of n= 2 technical replicate experiments.

(E) Bar graphs showing proliferation capacity of flow sorted populations of miR-126 biosensor vector transduced primary AML patient samples after recovery from NSG mice. The red crosses indicate the gated populations that were able to recapitulate the AML ΔNGFR/eGFP hierarchy in vivo. Data represents mean ± SEM of n= 2 technical replicate experiments.

Table S2, related to Figure 2. AML Patient Samples Used for miR-126 Biosensor Lentivector in vivo Studies.

AML	Sample Type	FAB	Age	Sex	Karyotype	Engraftment of AML Subpopulations			
						$CD34^+$ $CD38^-$	$CD34^+$ $CD38^+$	$CD34^-$ $CD38^+$	$CD34^-$ $CD38^-$
1	Relapse	Unclass	48	F	46,XX,t(2;21)(p21;q22)[4]/46,XX,9(1;21)(q22;q22)	+	+	-	-
3	Diagnosis	Unclass	52	F	47,XX,+8	+	+	+	+
7	Diagnosis	Unclass	47.9	M	n.d.	+	-	-	+
18	Diagnosis	M4	34.8	M	45,XY, inv(3)(q21q26.2) -7[20]	NT	NT	NT	NT

(+) symbols at right represent CD34/CD38 fractions that engraft immuno-deficient mice. (-) symbols represent fractions that were functionally evaluated and do not engraft immuno-deficient mice. (NT) symbols represent fractions that were not evaluated for LSC activity.

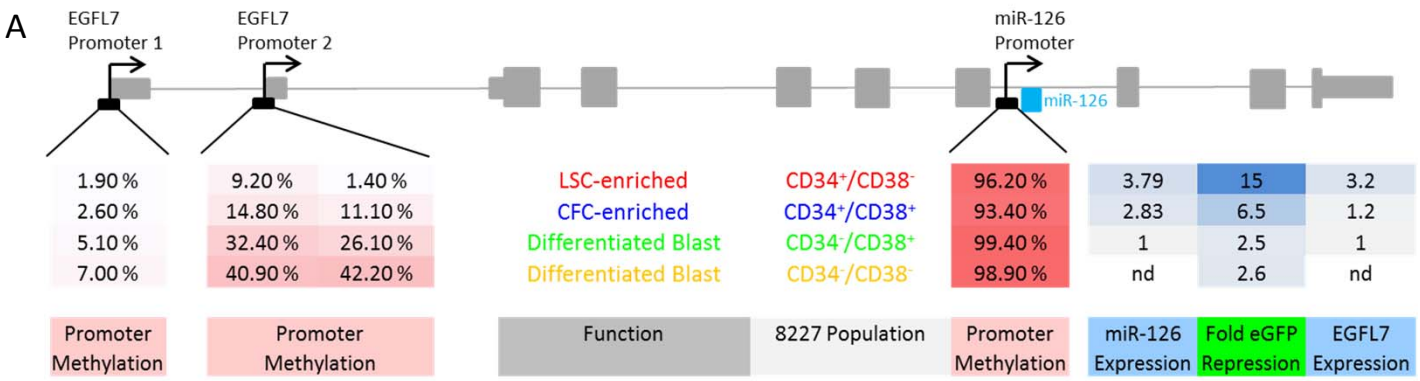
A
EGFL7 Promoter 1
EGFL7 Promoter 2
miR-126 Promoter
miR-126
1.90 %
2.60 %
5.10 %
7.00 %
9.20 %
14.80 %
32.40 %
40.90 %
1.40 %
11.10 %
26.10 %
42.20 %
LSC-enriched
CFC-enriched
Differentiated Blast
Differentiated Blast
CD34+/CD38-
CD34+/CD38+
CD34-/CD38+
CD34-/CD38-
96.20 %
93.40 %
99.40 %
98.90 %
3.79
2.83
1
nd
15
6.5
2.5
2.6
3.2
1.2
1
nd
Promoter Methylation
Promoter Methylation
Function
8227 Population
Promoter Methylation
miR-126 Expression
Fold eGFP Repression
EGFL7 Expression

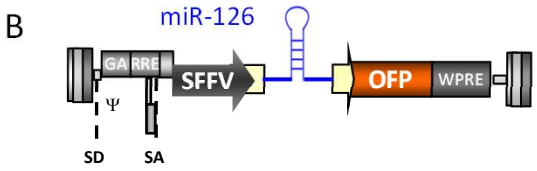
B
miR-126
GA
RRE
Ψ
SFFV
OFP
WPRE
SD
SA

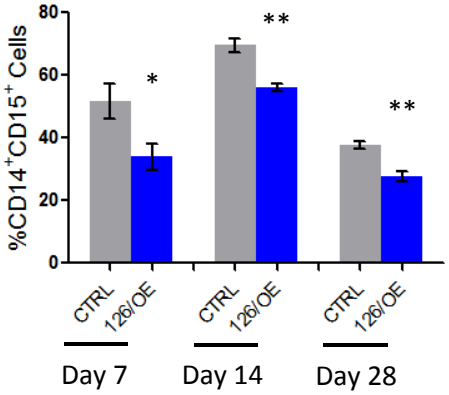
C
%CD14+CD15+ Cells
80
60
40
20
0
*
**
**
CTRL
126/OE
Day 7
Day 14
Day 28

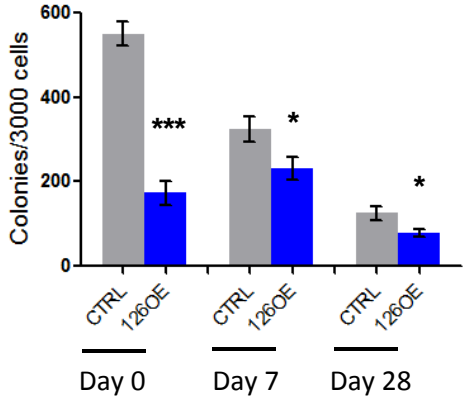
D
Colonies/3000 cells
600
400
200
0
***
*
*
CTRL
126OE
Day 0
Day 7
Day 28

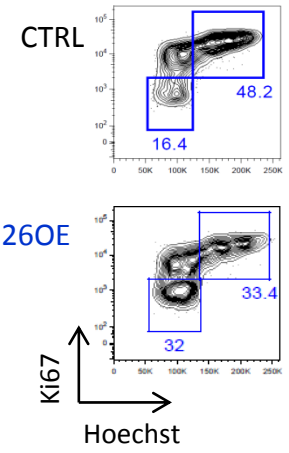
E
CTRL
48.2
16.4
126OE
33.4
32
Ki67
Hoechst

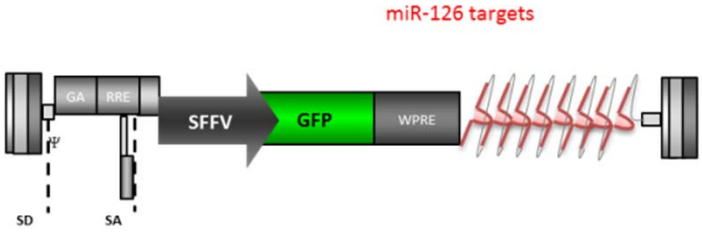
miR-126 targets
F
GA
RRE
Ψ
SFFV
GFP
WPRE
SD
SA

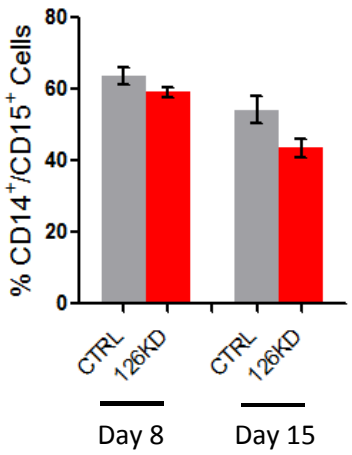
G
% CD14+/CD15+ Cells
80
60
40
20
0
CTRL
126KD
Day 8
Day 15

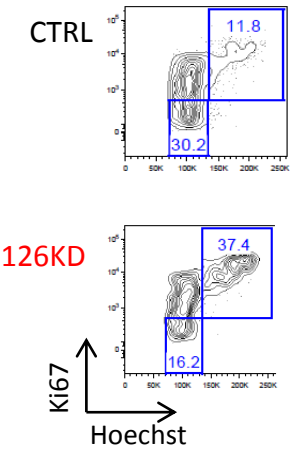
H
CTRL
11.8
30.2
126KD
37.4
16.2
Ki67
Hoechst

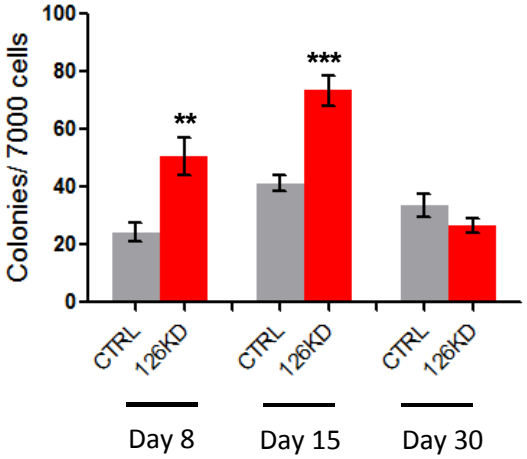
I
Colonies/ 7000 cells
100
80
60
40
20
0
**
***
CTRL
126KD
Day 8
Day 15
Day 30

Figure S3, related to Figure 3. Enforced expression and knockdown of miR-126 alters proliferation and differentiation status of primitive AML cells in vitro.

(A) Schematic of the EGFL7/miR-126 locus. Promoter methylation was determined by CD34/CD38 sorting of 8227 subpopulations. Methylated DNA immunoprecipitation (MeDIP) combined with tiling array hybridization. High methylation of the internal miR-126 promoter suggests that miR-126 expression is regulated from the EGFL7 promotor 2 site, which is progressively methylated with increasing differentiation of the 8227 cells. This differentiation is correlated with changes in cellular function as measured by in vitro culture initiation, in vivo leukemia initiation, colony forming capacity, and proliferation. Furthermore, miR-126 expression by array (normalized log2 transformed levels) and EGFL7 expression levels from array (normalized log2 transformed levels) are highest in the LSC enriched fraction and are progressively reduced with increasing differentiation. miR-126 bioactivity, as measured by the miR-126 biosensor vector, is highest in the LSC fraction and decreases with differentiation.

(B) Schematic representation of the lentiviral construct for enforced expression of miR-126. The human miR-126 hairpin is driven off of the SFFV promotor.

(C) 8227 leukemia cells were transduced with lentivectors expressing miR-126 (126OE) or an empty control vector (CTRL). Transduced cells were flow sorted for mOrange (mO^+) expression and plated in liquid culture conditions for 28 days with weekly passage. Graphical representation of the proportion of $CD14^+CD15^+$ in 8227 CTRL transduced cells or 126OE cells on days 7, 14 and 28 in post-sort cultures. Data represents mean $\pm$ SEM of n=3 replicate experiments where * $p < 0.05$, ** $p < 0.01$.

(D) Colony forming potential of CTRL and 126OE 8227 cells measured by methylcellulose CFC assay and evaluated a day 0, 7, and 28 of culture. Data represents mean $\pm$ SEM of n=2 technical replicate experiments where * $p < 0.05$, *** $p < 0.001$.

(E) Representative flow plots for cell cycle analysis with Hoechst and Ki67 cell staining of CTRL and 126/OE 8227 AML cells.

(F) Schematic representing the lentiviral sponge construct for knockdown of endogenous miR-126 activity. Eight imperfect miR-126 binding sites are cloned downstream of eGFP and driven off of an SFFV promotor.

(G) 8227 leukemia cells were transduced with lentivectors expressing miR-126 sponge (126KD) or an empty control vector (CTRL). Transduced cells were flow sorted for enhanced Green Fluorescent Protein ($eGFP^+$) expression and plated in liquid culture conditions for 30 days with weekly passage. Graph showing the proportion of $CD14^+CD15^+$ in 8227 CTRL transduced cells or 126KD cells at days 7 and 15 post-sort. Data represents mean $\pm$ SEM of n= 3 replicate experiments.

(H) Representative flow plots for cell cycle analysis with Hoechst and Ki67 cell staining of CTRL and 126KD 8227 AML cells.

(I) Graph showing colony forming potential of bulk miR-126KD 8227 cultures days 7, 15 and 30 after culture initiation. Data represents mean $\pm$ SEM of n= 3 replicate experiments where ** $p < 0.01$, *** $p < 0.001$.

A

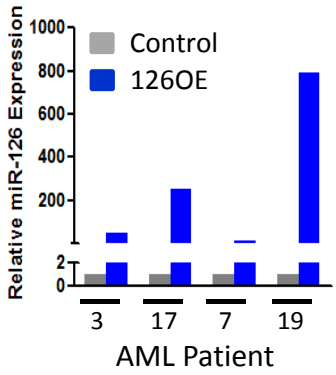

B

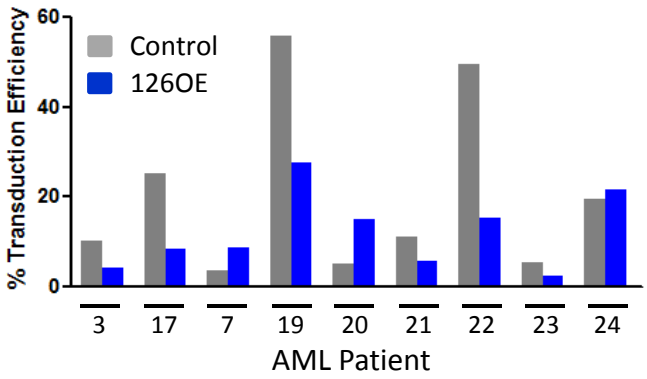

C

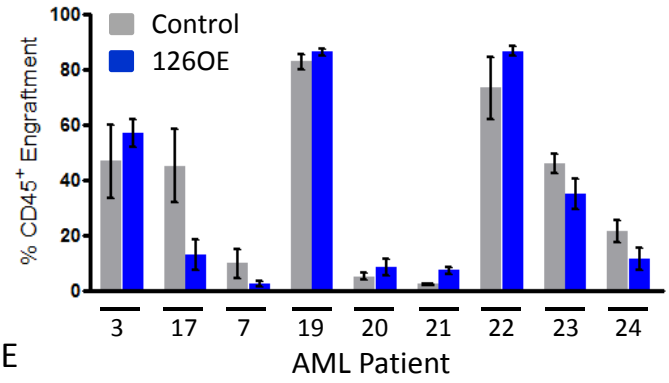

D

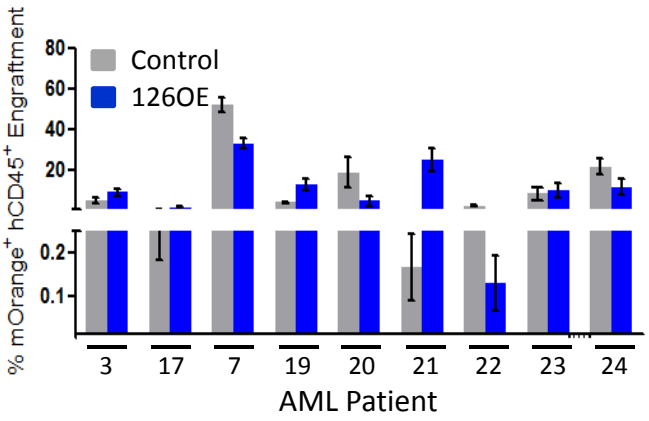

E

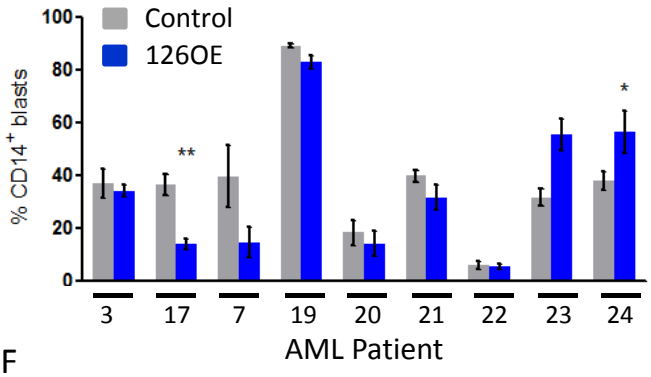

F

2° AML 3	# Cells Injected	% Mice Engrafted
CTRL	25,000	100% (2/2)
	5,000	0% (0/4)
	2,500	0% (0/5)
	500	0% (0/5)
126OE	25,000	100% (2/2)
	5,000	75% (3/4)
	2,500	0% (0/5)
	500	0% (0/5)

AML 17	# Cells Injected	% Mice Engrafted
CTRL	50,000	50% (1/2)
	25,000	0% (0/5)
	5,000	0% (0/5)
	1,000	0% (0/5)
126OE	50,000	100% (2/2)
	25,000	100% (5/5)
	5,000	80% (4/5)
	1,000	0% (0/5)

AML 7	# Cells Injected	% Mice Engrafted
CTRL	100,000	100% (2/2)
	25,000	20% (1/5)
	5,000	17% (1/6)
126OE	100,000	100% (4/4)
	25,000	100% (5/5)
	5,000	71% (5/7)

Group	Lower	Estimate	Upper
CTRL	103673	28175	7658
126OE	20845	8111	3156

Group	Lower	Estimate	Upper
CTRL	1587342	231601	33792
126OE	11021	4429	1780

Group	Lower	Estimate	Upper
CTRL	145005	52210	18799
126OE	9676	3942	1606

Figure S4, related to Figure 4. Increased miR-126 levels expand human AML LSC numbers in vivo.

(A) Relative levels of miR-126-3p expression for a subset of CTRL and 126/OE lentivirus transduced AML patient samples after 12 weeks in primary mice.

(B) Nine human AML samples were thawed, transduced overnight with lentiviruses expressing miR-126 (126/OE) or an empty vector (CTRL) and transplanted into NSG mice. After 12 weeks, mice were euthanized and bone marrow recovered for analysis. Percent AML cells transduced in 9 patient samples after overnight exposure to CTRL and 126/OE lentivirus (mOrange positivity) measured by flow cytometry 3 days post-virus transduction.

(C) Bar graph depicting changes in $hCD45^+$ levels within the bone marrow of transplanted mice after enforced expression of miR-126. Data shown represent the mean $\pm$ SEM of 4-6 mice

(D) Graphical representation of the proportion of mO^+hCD45^+cells in the bone marrow of CTRL and 126OE AML samples after 12 weeks. Data shown represent the mean $\pm$ SEM of 4-6 mice

(E) Graph of the proportion of $CD45^+mO^+CD14^+$ cells in the bone marrow of CTRL and 126OE AML samples after 12 weeks. Data shown represent the mean $\pm$ SEM of 4-6 mice where * $p < 0.05$, ** $p < 0.01$.

(F) Transduced human $CD45^+mO^+$ AML cells were flow sorted from primary mice and transplanted into secondary recipients for 8-10 weeks at limiting doses. Human $CD45^+$ marking > 0.5% was considered positive for AML engraftment. Human grafts were confirmed to be $CD33^+CD19^-$ AML. Tables depict transplanted cell numbers, engrafted mice percentages and numbers per CTRL and 126OE group for each AML patient sample.

Table S3, related to Figure 4. AML Patient Samples Used for in vivo Functional Evaluation of miR-126.

AML	Sample Type	FAB	Age	Sex	Karyotype	Engraftment of AML Subpopulations			
						$CD34^+$ $CD38^-$	$CD34^+$ $CD38^+$	$CD34^-$ $CD38^+$	$CD34^-$ $CD38^-$
17	Diag	Unclass	42.7	M	46, XY	+	+	+	+
19	Diag	Unclass	37.5	F	46,XX[18]: NPM1c+, FLT3-ITD+	+	+	-	+
20	Diag	M5a	60	M	45,X,-Y,t(11:19)(q23;p13.1)[20]	+	-	+	+
21	Diag	Unclass	31.5	F	46,XX,t(9;11)(p22;q23){[0]	NT	NT	NT	NT
22	Refractory	Unclass	36.7	M	46,XY,t(1;3)(q32;q26~27),del(20)(q13.1)[11]	NT	NT	NT	NT
23	Diag	M4	33.4	M	46,XY[20]; NPM1c+, FLT3-ITD+	NT	NT	NT	NT
24	Refractory	Unclass	70.7	F	46,XX,t(1;14)(q21;q11.2)[20]	NT	NT	NT	NT

(+) Symbols at right represent CD34/CD38 fractions that engraft immuno-deficient mice. (-) symbols represent fractions that were functionally evaluated by transplantation, but do not engraft immuno-deficient mice. (NT) symbols represent fractions that were not evaluated for LSC activity.

A

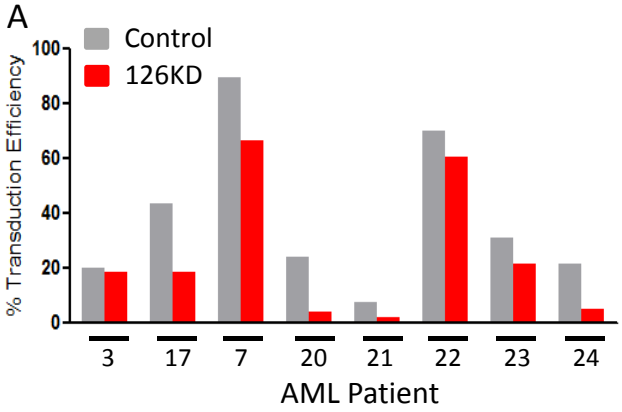

B

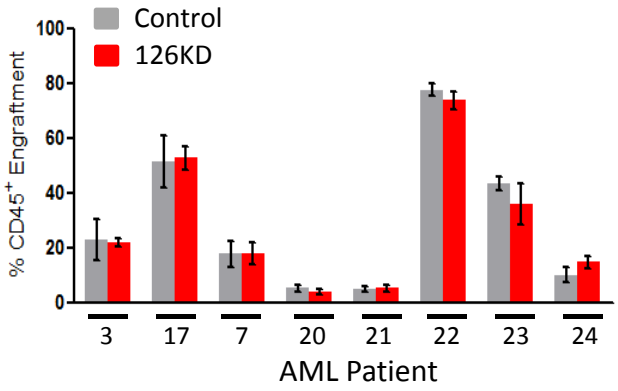

C

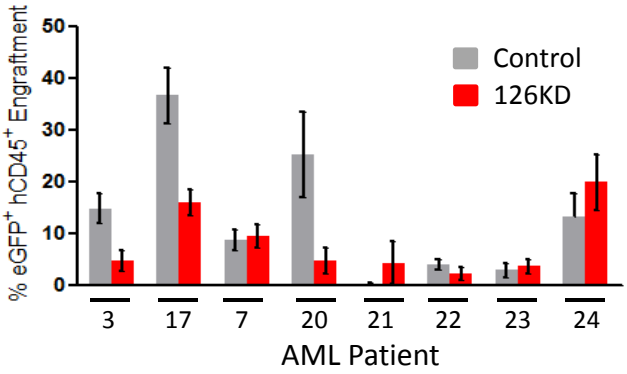

D

2°

AML 3	# Cells Injected	% Mice Engrafted
CTRL	625,000	100% (1/1)
	125,000	100% (5/5)
	25,000	100% (5/5)
	5,000	100% (4/4)
126KD	625,000	100% (2/2)
	125,000	100% (3/3)
	25,000	100% (5/5)
	5,000	0% (0/4)

Group	Lower	Estimate	Upper
CTRL	11524	3563	1102
126KD	31959	12615	4980

~3.47 Fold Decrease
In Frequency
p = 0.0087

AML 17	# Cells Injected	% Mice Engrafted
CTRL	300,000	100% (1/1)
	150,000	100% (4/4)
	75,000	100% (2/3)
126KD	300,000	100% (3/3)
	150,000	75% (3/4)
	75,000	0% (0/3)

Group	Lower	Estimate	Upper
CTRL	134514	49930	18533
126KD	197916	84804	36337

~1.7 Fold Decrease
In Frequency
p = 0.119

AML 7	# Cells Injected	% Mice Engrafted
CTRL	500,000	50% (2/1)
	250,000	100% (2/2)
	100,000	50% (2/4)
	25,000	0% (0/1)
126KD	500,000	50% (1/2)
	250,000	0% (0/1)
	100,000	75% (3/4)
	25,000	50% (1/2)

Group	Lower	Estimate	Upper
CTRL	646891	238740	88109
126KD	695315	239104	82223

No Fold Change
In Frequency
p = 0.998

Figure S5, related to Figure 5. Diminished miR-126 levels reduce the proportion of primitive AML cells

(A) Eight human AML samples were thawed, transduced overnight with lentiviruses expressing a miR-126 sponge (126KD) or an empty vector (CTRL) and transplanted into NSG mice. After 12 weeks, mice were euthanized and bone marrow recovered for analysis. Percent AML cells transduced in 8 patient samples after overnight exposure to CTRL and 126KD lentivirus (eGFP positivity) measured by flow cytometry 3 days post-virus transduction.

(B) Bar graph depicting changes in $hCD45^+$ levels within the bone marrow of transplanted mice with reduced expression of miR-126. Data shown represent the mean $\pm$ SEM of 4-6 mice.

(C) Proportional levels of $eGFP^+hCD45^+$cells in the bone marrow of CTRL and 126KD AML samples after 12 weeks. Data shown represent mean $\pm$ SEM of 4-6 mice.

(D) LSC frequency upon 126KD. Transduced human $CD45^+eGFP^+$ AML cells were flow sorted from primary mice and transplanted into secondary recipients for 8-10 weeks at limiting doses. Human $CD45^+$ marking >0.5% was considered positive for AML engraftment. Human grafts were confirmed to be $CD33^+CD19^-$ AML. Tables depict transplanted cell numbers, engrafted mice percentages and numbers per CTRL and 126KD group for each AML patient sample.

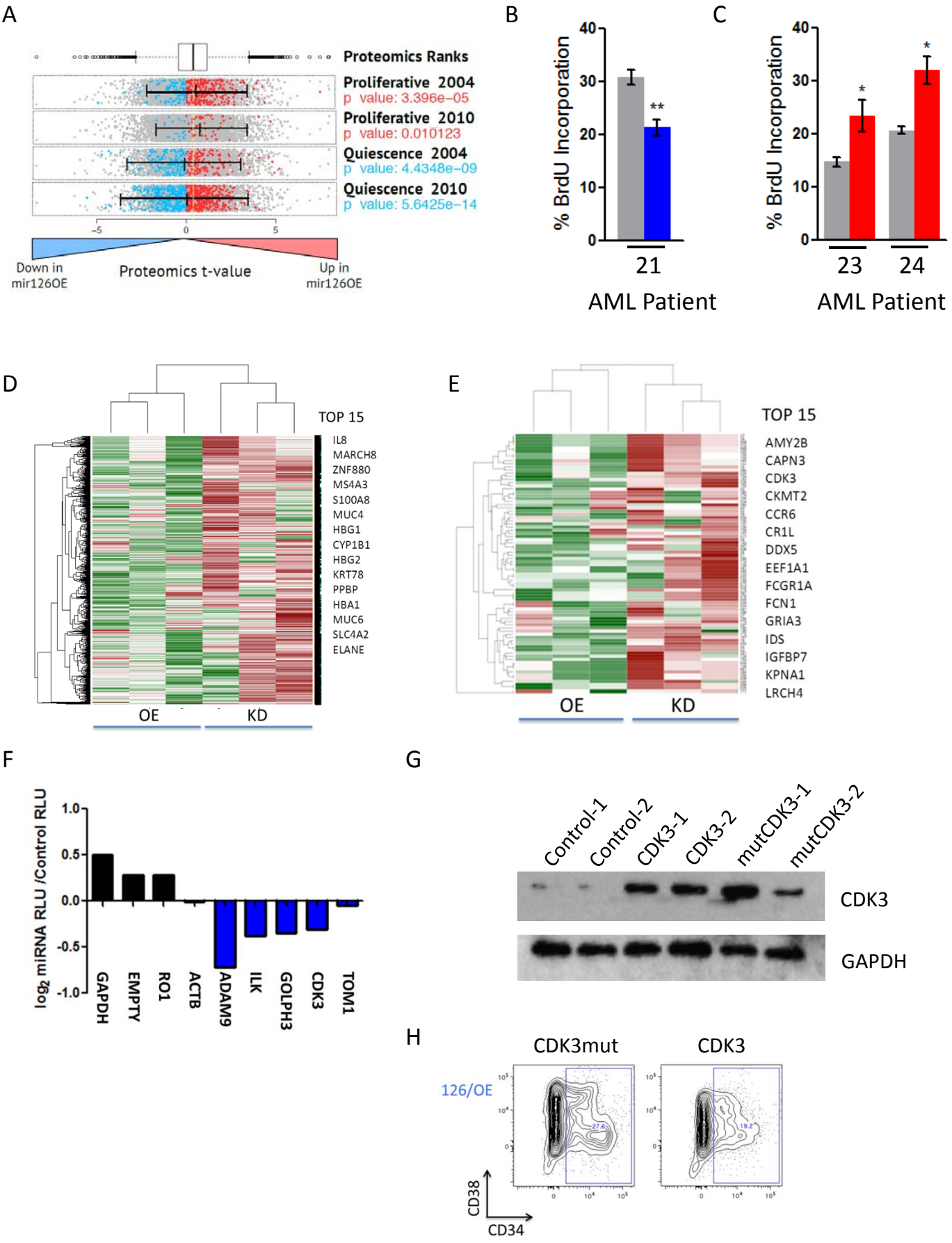
A
Proteomics Ranks
Proliferative 2004
p value: 3.396e−05
Proliferative 2010
p value: 0.010123
Quiescence 2004
p value: 4.4348e−09
Quiescence 2010
p value: 5.6425e−14
−5
0
5
Down in mir126OE
Proteomics t-value
Up in mir126OE
B
% BrdU Incorporation
40
30
20
10
0
**
21
AML Patient
C
% BrdU Incorporation
40
30
20
10
0
*
*
23
24
AML Patient
D
TOP 15
IL8
MARCH8
ZNF880
MS4A3
S100A8
MUC4
HBG1
CYP1B1
HBG2
KRT78
PPBP
HBA1
MUC6
SLC4A2
ELANE
OE
KD
E
TOP 15
AMY2B
CAPN3
CDK3
CKMT2
CCR6
CR1L
DDX5
EEF1A1
FCGR1A
FCN1
GRIA3
IDS
IGFBP7
KPNA1
LRCH4
OE
KD
F
log2 miRNA RLU /Control RLU
1.0
0.5
0.0
-0.5
-1.0
GAPDH
EMPTY
RO1
ACTB
ADAM9
ILK
GOLPH3
CDK3
TOM1
G
Control-1
Control-2
CDK3-1
CDK3-2
mutCDK3-1
mutCDK3-2
CDK3
GAPDH
H
CDK3mut
CDK3
126/OE
27.6
19.2
CD38
CD34

Figure S6, related to Figure 6. miR-126 targets CDK3 in primitive AML cells and enforced expression can rescue the 126OE phenotype in vitro

(A) Comparison of the proteomics data against published quiescent/proliferative signatures. For the proliferative gene sets, Mann Whitney non-parametric analysis was used to test the significance of the overlap between the published proliferative signatures and the proteomic gene set that was up-regulated in miR-126OE. For the quiescent gene sets, Mann Whitney non-parametric analysis was used to look for significance of the overlap between the quiescent signature and proteomic gene set that was down-regulated in miR-126OE. Grey dots represent all the different proteomics ranks t values. Red dots represent proteins found in the gene set of interest with a t-value greater than 0. Blue dots represent proteins found in the gene set of interest with a t value less than 0. The p value indicated below each gene set is the most significant Wilcox p value from the two scenarios tested, "greater" (red), "less" (blue). The yellow dotted line shows the mean of the proteomic ranks t-values.

(B) Human AML samples were thawed, transduced overnight with lentiviruses expressing miR-126 (126OE), a miR-126 sponge (126KD) or an empty vector (CTRL) and transplanted into NSG mice for 8-12 weeks. Sixteen hours prior to mouse euthanization, 1 mg BrdU in 200µl of sterile PBS was IP injected into each mouse. Bone marrow was recovered and processed for analysis. Graph showing proliferation measured by BrdU incorporation assay of CTRL or 126OE transduced AML cells in vivo. Data is shown as mean ± SEM of 5 replicate animals where ** $p<0.01$.

(C) Proliferation measured by BrdU incorporation assay of CTRL or 126KD transduced AML cells in vivo. Data is shown as mean ± SEM of 5 replicate animals where * $p<0.05$.

(D) Heat map ranking all genes that significantly increased in expression with miR-126KD and decreased in expression after miR-126OE in primitive 8227 AML cells. Green indicates decreased expression, red indicates increased expression upon miR-126 modulation. Columns indicate three replicate experiments.

(E) Heatmap of 84 miR-126 predicted targets listed in descending order of level of increase after 126KD. Green indicates decreased expression, red indicates increased expression upon miR-126 modulation. Columns indicate three replicate experiments. Note that CDK3 is near the top of listed targets.

(F) Validation of miR-126 predicted targets by luciferase 3' UTR reporter assay.

(G) Construction and functional validation of CDK3OE and control CDK3mutOE (kinase mutant) vectors. Western blot analysis shows high expression of CDK3 and mutCDK3 7 days post transduction of 8227 cells.

(H) CDK3OE rescue of $CD34^+$ cell expansion upon 126OE. The percentage of $CD34^+$ cells in double transduced cultures is shown as representative flow plots.

Table S4, related to Figure 6. Table S4 is provided as an Excel file

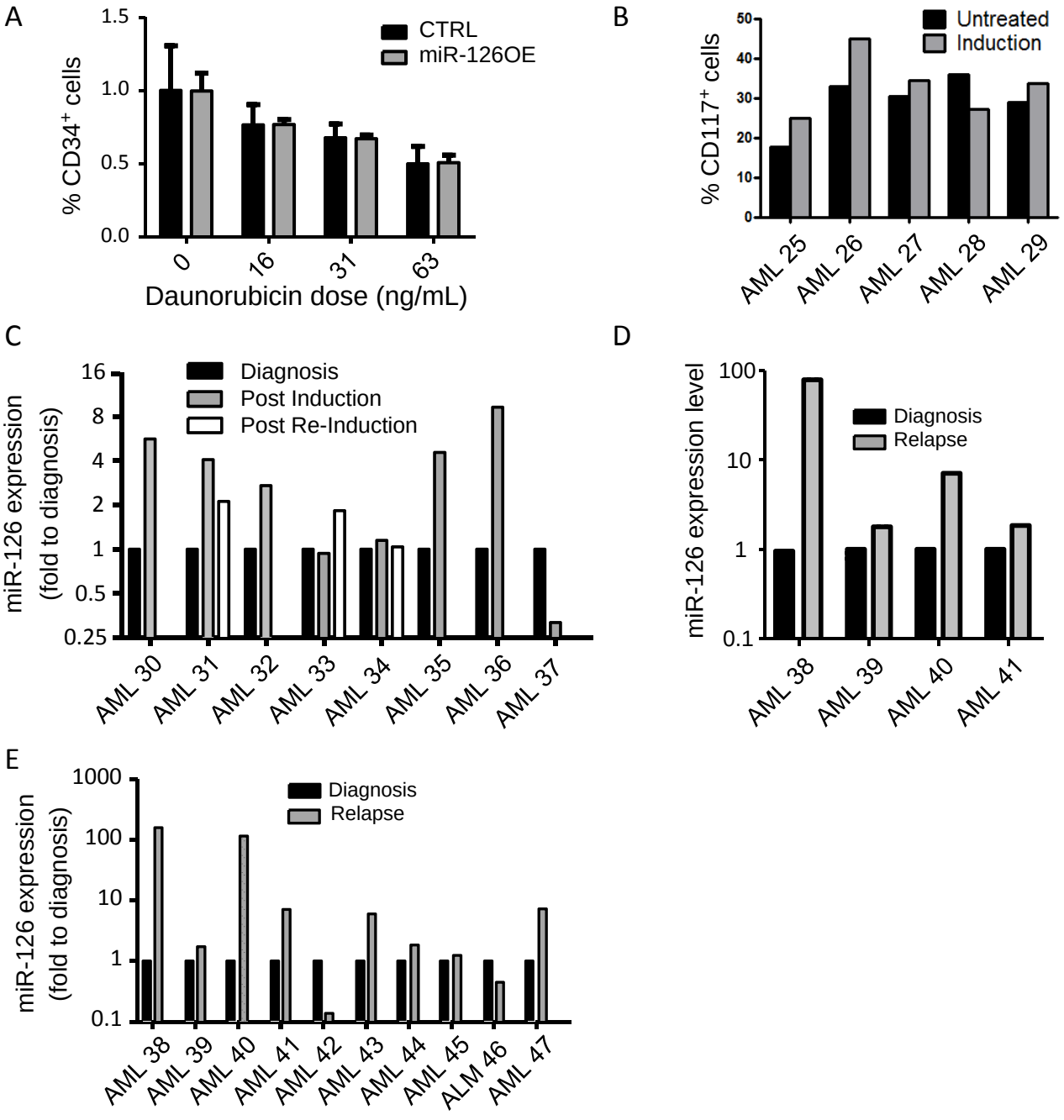
A
% CD34+ cells
1.5
1.0
0.5
0.0
CTRL
miR-126OE
0
16
31
63
Daunorubicin dose (ng/mL)
B
% CD117+ cells
50
40
30
20
10
0
Untreated
Induction
AML 25
AML 26
AML 27
AML 28
AML 29
C
miR-126 expression
(fold to diagnosis)
16
8
4
2
1
0.5
0.25
Diagnosis
Post Induction
Post Re-Induction
AML 30
AML 31
AML 32
AML 33
AML 34
AML 35
AML 36
AML 37
D
miR-126 expression level
100
10
1
0.1
Diagnosis
Relapse
AML 38
AML 39
AML 40
AML 41
E
miR-126 expression
(fold to diagnosis)
1000
100
10
1
0.1
Diagnosis
Relapse
AML 38
AML 39
AML 40
AML 41
AML 42
AML 43
AML 44
AML 45
ALM 46
AML 47

Figure S7, related to Figure 7. High expression of miR-126 protects primitive AML cells from chemotherapy and is a biomarker of refractory LSC.

(A) Graphical representation of non-transduced $CD34^+$ 8227 cells with increasing doses of Daunorubicin. Bars represent mean ± SEM of 3 independent cultures with 10 replicate wells each.

(B) Primary patient AML cells were plated onto MS5 stroma, after 24 hours cells were treated with vehicle or with Daunorubicin/AraC for 72 hours. Cells were recovered and evaluated for live cell content and immuno-phenotype by flow cytometry. Graphical representation of flow cytometry results of chemotherapy treated AML stromal cultures shows an increase in $CD117^+$ AML blasts after 72 hour treatment with Daunorubicin/AraC.

(C) miR-126 levels in 8 individual AML patients who failed to achieve complete remission (CR) after anthracycline/cytarabin induction chemotherapy. qPCR was performed on $CD45^{dim}$ sorted blasts from 8 patient samples at diagnosis (n=8, day 0) and, at day 14 (n=4) and day 30 (n=5) after initiation of induction chemotherapy, as well as on day 30 after (unsuccessful) salvage chemotherapy (n=3).

(D-E) Levels of miR-126 in individual paired diagnosis/relapse AML patient samples. AML patient samples were thawed and sorted for $CD45^{dim}$ or $CD45^{dim}CD117^+$ or $CD45^{dim}CD34^+$ populations. qPCR was used to evaluate the relative levels of miR-126 in paired patient samples. Graphical representation of miR-126 levels in $CD45^{dim}$ (D) and $CD45^{dim}CD117^+$ (samples 38-45) and $CD45^{dim}CD34^+$ (samples 46-47) (E) AML blasts in paired diagnosis/relapse samples.

Table S5, related to Figure 7. Clinical and Molecular Characteristics of AML Patients

AML	Age	Sex	De novo/Secondary	FAB	WBC	Cytogenetics	NPM1 mutation status	FLT3-ITD mutation status
AML Samples used in Stromal Assay								
25	72	M	sAML	n.d.	43	45,X,-Y[20]	n.d.	n.d.
26	28	F	de novo	M1	105.8	46,XX[20]	(+)	(-)
27	58	F	de novo	M5	35.6	46,XX[20]	(+)	(+)
28	50	M	de novo	M4Eo	41.3	46, XY, inv(16)(p13.1q22)[17]/47,idem,+22[3]	n.d.	n.d.
29	67	F	de novo	M1	128	46,XX[20]	n.d.	n.d.
Diagnosis/Refractory AML Patient Sample Pairs								
30	72	M	de novo	M2	41.8	46,XY T(10;13)(q24;q22)[20]	(+)	(+)
31	67	M	sAML	M4Eo	3.7	46,XY[20]	(+)	(-)
32	72	M	de novo	M5B	6.1	Complex/Pseudodiploid	(-)	(-)
33	48	M	de novo	M2	5	46,XY[20]	(-)	(-)
34	42	M	sAML	M2	2.4	Complex	(-)	(-)
35	50	M	de novo	M1	116.9	46,XY[20]	(+)	(+)
36	68	M	de novo	M2	2.1	46,XY[20]	(+)	(-)
37	37	F	de novo	M2	60	46,XX[20]	(+)	(+)
Diagnosis/Relapse AML Patient Sample Pairs								
38	75	M	de novo	M1	60	46,XY[20]	(+)	(-)
39	43	M	de novo	M4Eo	55	46,XY[20]	(+)	(-)
40	60	M	de novo	M4Eo	108	46,XY[20]	(+)	(-)
41	60	M	sAML	M5a	134	45,X,-Y,t(11;19)(q23;p13.1)[20]	n.d.	n.d.
42	27	F	de novo	M2	150	n.d.	(-)	(-)
43	77	M	de novo	M2/M4	215	n.d.	(-)	(+)
44	77	M	de novo	M5	73.9	46,XY[20]	(+)	(+)
45	49	F	de novo	M2	n.d.	46,XX, t(8;11)(q24.2-3;q1)[20]	(+)	(+)
46	72	F	de novo	M4	11.6	46,XX[20]	(-)	(-)
47	52	F	de novo	M4	56.7	46,XX[20]	(-)	(-)

Clinical parameters of the AML patient bone marrow samples used for in vitro stromal chemotherapy assay (AML 19 to AML 23), AML patient cohort that failed to achieve complete remission (AML 24 to AML 31), and paired diagnosis/relapse AML patient samples (AML32 to AML 41).

SUPPLEMENTAL EXPERIMENTAL PROCEDURES

Limiting dilution analysis

$CD45^+mO^+$ (miR-126OE) or $CD45^+eGFP^+$ (miR-126KD) cells from pooled bone marrow (BM) of primary mice 12 weeks after transplantation and injection of various cell doses into conditioned secondary recipients. A secondary mouse was scored as positive if it had >0.5% BM engraftment 12 weeks after transplantation. Leukemia stem cell (LSC) frequency was estimated by linear regression analysis and Poisson statistics using publicly available ELDA (Extreme Limiting Dilution Analysis, http://bioinf.wehi.edu.au/software/elda/) software (Hu and Smyth, 2009).

Nanostring miRNA data generation and processing

The expression of 30 miRNAs from 74 acute myeloid leukemia (AML) samples from Princess Margaret Cancer Centre (PMCC) were measured and normalized using the NanoString platform (Geiss et al., 2008). For the TCGA cohort, miRNA-Seq RPM (i.e., reads per million) normalized profiles generated using the Illumina Genome Analyzer, which captured the expression of ~492 miRNAs, were downloaded from the TCGA data portal (Cancer Genome Atlas Research Network, 2013). The maximum linear expression of 29 mature miRNAs that were common to both datasets was analyzed in this study. All miRNA expression values were increased by one plus a small normally distributed random value to produce non-zero expression profiles. These profiles were then $\log_2$ transformed and filtered for miRNAs with high variance (i.e., values outside of the 20^{th} to 80^{th} percentile range). Finally, ComBat normalization was applied to reduce the cross-platform differences (i.e., batch effects) between the 2 datasets (Johnson et al.,

2007)(Fei et al., 2013)(Rudy and Valafar, 2011)(Sirinukunwattana et al., 2013). All data analysis was done in R 2.15.2.

Building prognostic miRNA signatures

The glmnet 1.9-3 R package was configured for L1 regularized Cox regression, enabled with leave one out cross validation. This statistical learning tool was then applied to the PMCC dataset to select a minimal weighted combination of miRNA expression that best explained patient survival time. This training phase resulted in a 4-miRNA signature that was tested for prognostic value in the TCGA dataset. Per-patient risk scores were computed using dot products between the expression of signature miRNAs (i.e., c_i) and their corresponding regression coefficients (i.e., weights w_i) as follows: $(w_1 \times c_1) + (w_2 \times c_2) + (w_3 \times c_3) + \ldots$ etc. The resulting continuous scores were further discretized based on the 50th percentile (i.e., median) split, where patients with scores above the split were considered to be at high risk (else low risk) as previously described (Eppert et al., 2011).

miRNA signature performance

In survival analysis, overall survival (OS) was defined as the time from AML diagnosis until death from any cause, event-free survival (EFS) was defined as the time from AML diagnosis until induction failure, relapse, or death from any cause, and relapse-free survival (RFS) defined as the time from the date of first complete remission (CR1) until relapse or death, regardless of cause (Cheson et al., 2003). The survival 2.37-4 package in R (Borgan, 2001) was used to assess the prognostic value of the miRNA signature scores computed for each patient in the TCGA dataset. Survival differences between patients with low- and high- signature scores were assessed using uni- and multi- variate Cox proportional hazards (CPH) and Kaplan-Meier models. In the multivariate case, the prognostic impact of white blood count (WBC), gene mutational status

(i.e., *NPM1*, *FLT3*ITD), age, type of AML onset (i.e., de-novo, secondary), and cytogenetic risk group (i.e., favorable, intermediate, or adverse) served as controls based on their established prognostic relevance in AML and patient data availability (Cancer Genome Atlas Research Network, 2013)(Eppert et al., 2011). The proportional hazards assumption was tested by examining Schoenfeld residuals for each patient parameter (e.g., WBC, age) used in the survival models. Parameters that significantly ($p<0.05$) violated this assumption were used to construct a stratified CPH model to remove their non-proportionality effects on hazard. Signature performance was assessed based on: (1) the lower 95% confidence interval of the signature scores' hazard ratio being greater than the value of one in multivariate survival analysis ($p< 0.05$, Wald test); and (2) the ability of the signature scores to significantly dichotomize low- from high- risk patients in univariate survival models ($p<0.05$, log rank test).

Illumina Microarray

8227 cells were transduced with miR-126/OE or miR-126/KD vectors or their respective empty control lenti-vectors at a multiplicity of infection (MOI) of 30. Cells were expanded under standard culture conditions for two weeks post-transduction and then flow sorted into $CD34^{+}CD38^{-}$, $CD34^{+}CD38^{+}$ and $CD34^{-}CD38^{+}$ populations. Recovered cells were stored in Trizol (Invitrogen) at -80^{o}C. RNA from transduced 8227 cells was extracted using Trizol (Invitrogen) and gene expression assayed on HT-12_v4 microarrays (Illumina). Quantile normalization was performed and probes were filtered by detection p-value (<0.1) (GeneSpring GX, Agilent). Next, to remove uninformative probes, those that did not exceed a threshold of 7.8 in all replicates of any one condition were eliminated, leaving 15812 probes for analysis.

Gene set enrichment analysis

Gene set enrichment analysis was performed using g:Profiler software with the options significant only, ordered query on 2564 genes selected based both on a positive log fold change (logFC) in 8227 126/KD and a negative logFC in 8227 126/OE versus Control samples (Reimand et al., 2011). Gene-sets with a size equal or greater than 500 were removed. Results were visualized using Cytoscape 2.8.1 (Smoot et al., 2011) and an enrichment map (version 1.2 of Enrichment Map software (Merico et al., 2010) was generated using enriched gene-sets with a p-value <0.05 and overlap coefficient set of 0.5.

Mass Spectrometry Sample Preparation

One to two weeks post viral transduction, 8227 cells with miR-126 overexpression (126/OE) and control vector (CTRL) were counted and washed twice with ice-cold PBS. 100,000 cells for each experimental condition, in biological triplicate, were subjected to sample preparation similar to (Kulak et al., 2014). Cells were lysed using 50 µl of lysis buffer (consisting of 6 M Guanidinium Hydrochloride, 10 mM TCEP, 40 mM CAA, 100 mM Tris pH8.5). Samples were boiled at 95^{o}C for 5 minutes, after which they were sonicated on high for 3x 10 seconds in a Bioruptor sonication water bath (Diagenode) at 4^{o}C. Samples were diluted 1:3 with 10% Acetonitrile, 25 mM Tris pH 8.5, LysC (MS grade, Wako) was added in a 1:50 (enzyme to protein) ratio, and samples were incubated at 37^{o}C for 4hrs. Samples were further diluted to 1:10 with 10% Acetonitrile, 25 mM Tris pH 8.5, trypsin (MS grade, Promega) was added in a 1:100 (enzyme to protein) ratio and samples were incubated overnight at 37^{o}C. Enzyme activity was quenched by adding 2% trifluoroacetic acid (TFA) to a final concentration of 1%. Prior to mass spectrometry analysis, the peptides were fractionated using Strong Cation Exchange (SCX) in StageTip format. For each sample, 6 discs of SCX material (3M Empore) were packed in a 200ul tip, and the SCX material activated with 80 µl of 100% Acetonitrile (HPLC grade, Sigma). The tips were

equilibrated with 80 µl of 0.2% TFA, after which the samples were loaded using centrifugation at 4,000x rpm. After washing the tips twice with 100µl of 0.2% TFA, five initial fractions were eluted into clean 500µl Eppendorf tubes using 50, 75, 125, 200 and 300mM ammonium acetate, 20% Acetonitrile, 0.5% formic acid respectively. The final fraction was eluted using 5% ammonium hydroxide, 80% Acetonitrile. The eluted fractions were frozen on dry ice and concentrated in an Eppendorf Speedvac, and re-constituted in 1% TFA, 2% Acetonitrile for Mass Spectrometry (MS) analysis.

Mass Spectrometry Acquisition

For each SCX fraction, peptides were loaded onto a 50cm C18 reverse-phase analytical column (Thermo EasySpray ES803) using 100% Buffer A (0.1% Formic acid in water) at 750bar, using the Thermo EasyLC 1000 µHPLC system in a single-column setup and the column oven operating at 45°C. Peptides were eluted over a 140 minute gradient ranging from 5 to 48% of 100% acetonitrile, 0.1% formic acid at 250 nl/min, and the Orbitrap Fusion (Thermo Fisher Scientific) was run in a 3 second MS-OT, ddMS2-IT-HCD top speed method. Full MS spectra were collected at a resolution of 120,000, with an AGC target of 4×10^5 or maximum injection time of 50ms and a scan range of 400–1500m/z. Ions were isolated in a 1.6m/z window, with an AGC target of 1×10^4 or maximum injection time of 50ms, fragmented with a normalized collision energy of 30 and the resulting MS2 spectra were obtained in the ion trap. Dynamic exclusion was set to 60 seconds, and ions with a charge state <2, >7 or unknown were excluded. MS performance was verified for consistency by running complex cell lysate quality control standards, and chromatography was monitored to check for reproducibility. Each sample was run in technical duplicate and biological triplicate, and the reproducibility of the analyses is depicted in **Table S4**. The mass spectrometry data have been deposited to the ProteomeXchange

Consortium (http://proteomecentral.proteomexchange.org) via the PRIDE partner repository with the dataset identifier PXD001994 (username: reviewer02600@ebi.ac.uk, password: aLahIn44)(Hermjakob and Apweiler, 2006).

Label-free Quantitative Proteomics Analysis

The raw files were analyzed using MaxQuant version 1.5.2.8 (Cox and Mann, 2008) and standard settings. Briefly, label-free quantitation (LFQ) was enabled with a requirement of 3 unique peptides per protein. Variable modifications were set as Oxidation (M), Acetyl (protein N-term), Gln->pyro-Glu and Glu->pyro-Glu. Fixed modifications were set as Carbamidomethyl (C), false discovery rate was set to 1% and "match between runs" was enabled. The resulting protein groups file, containing all the LFQ intensities across all the samples was processed in Perseus (filtering for contaminants and reverse hits), resulting in 8,848 proteins identified in total, and 4,837 proteins quantified across all samples. To determine those proteins that are significantly different between 126OE and CTRL samples, the ratios of 126OE vs CTRL were calculated in each biological repeat and subjected to statistical analysis in Limma (R Statistical Framework) with Benjamini-Hochberg adjustment. This table is included as **Table S4**, and was used as input for downstream analysis with GSEA.

Proteomics

MaxQuant LFQ (Cox and Mann, 2008) intensities were used as a measure of protein expression in 8227 126OE and control samples. The entire protein expression set consisting of 3 biological replicates for each treatment group and corresponding technical replicates (total of 12 samples) was quantile normalized in R (R version 3.1.1) using the normalizer package (version 1.0). The normalized protein expression was further filtered to contain only proteins that had at least two measurements in either treatment or control.

Difference in protein expression between the groups was assessed using a moderated t-test available in the bioconductor limma package (version 3.20.9). P-values were further corrected to control for multiple hypothesis testing using the Benjamini-Hochberg procedure. 638 proteins had significant differential expression with nominal p-value <0.05, of those 451 were upregulated (t>0) and 187 were downregulated (t<0). Proteins and their corresponding t-statistic were used to create a rank file to be used in pathway analysis described below.

Pathway Analysis on the proteomics data

Gene Set Enrichment Analysis (Subramanian et al., 2005) was performed using the protein expression ordered from largest to smallest t statistics with parameters set to 1000 gene-set permutations and gene-sets size between 5 and 500. The gene-sets included for the GSEA analyses were obtained from KEGG, MsigDB-c2, NCI, Biocarta, IOB, Netpath, HumanCyc, Reactome, Panther and Gene Ontology (GO) databases, updated December 24, 2014 (http://download.baderlab.org/EM_Genesets/). An enrichment map (version 2.1.0 of Enrichment Map software (Merico et al., 2010) was generated using Cytoscape 3.2.1 using significantly enriched gene-sets with a nominal p-value <0.05 and FDR <0.01. Similarity between gene-sets was filtered by Jaccard coefficient >0.25. Only gene-sets enriched in downregulated proteins were further analyzed and visualized.

Correlation between miR-126 predicted targets and the proteomics modulated pathway

Four databases were used to create a list of miR-126 predicted targets (DIANA microT, picTar, TargetScan from the miRbase website (http://www.mirbase.org)) and miRanda from the microCosm website (http://www.ebi.ac.uk/enright-srv/microcosm/htdocs/targets/v5/). Downregulated predicted targets were compared to enriched gene-sets in the enrichment map and significance of overlap was scored using 2 statistical tests (a hypergeometric test and a one-

sample Wilcoxon rank sum test) so that highest significance corresponds to higher number of genes in each overlap relative to gene-set size (hypergeometric test) and proteins in the overlap showing the highest differential expression amplitude (one sample Wilcoxon test).

Correlation between the transcriptomic data and the proteomic modulated pathways

2564 genes were selected based both on a positive log fold change (logFC) in 8227 126KD and a negative logFC in 8227 126OE versus control samples. The list was ranked by the 8227 126KD logFC in a decreasing order and compared to enriched gene-sets in the enrichment map and significance of overlap was scored using 3 statistical tests (one hypergeometric test, two one-sample Wilcoxon rank sum tests) so that highest significance corresponds to a higher number of genes in each overlap relative to gene-set size (Hypergeometric test), genes in the overlap showing higher differential expression amplitude (one sample Wilcoxon test), and proteins in the overlap showing higher differential expression amplitude (one sample Wilcoxon test).

Correlation of the miR-126 predicted targets and the miR-126 modulated pathways

Four databases were used to create a list of miR-126 predicted targets (DIANA microT, picTar, TargetScan from the miRbase website (http://www.mirbase.org)) and miRanda from the microCosm website (http://www.ebi.ac.uk/enright srv/microcosm/htdocs/targets/v5/). 84 predicted targets were part of the 2564 genes up-regulated in 8227 126KD and down-regulated in 8227 126OE. This list was compared to enriched gene-sets in the enrichment map and overlap was scored using Fisher's Exact Test p-value. Overlaps with p-value <0.05 were visualized.

Global miRNA Profiling

As described in (Eppert et al., 2011), cells from 16 AML patients (**Figure S1A**) were stained with antibodies to cell surface markers CD34 and CD38 and flow sorted into $CD34^{+}CD38^{-}$,

$CD34^+CD38^+$, $CD34^-CD38^+$ and $CD34^-CD38^-$ populations. Three independent pooled cord blood samples from 15–22 donors were used for isolation of HSC subsets and progenitors. Representative sorting gates are in **Figure 1A**.

NSG mice 8–13 weeks old were pretreated with 2.75–3.4 Gy radiation before being injected intra-femorally with AML cells at a dose of 200 to 2.87×10^6 sorted cells per mouse, as described (Eppert et al., 2011). Mice were killed at 12 weeks (mean 10 weeks), and bone marrow from the injected right femur, opposite femur and, in some cases, both tibias and spleen were collected for flow cytometry and secondary transplantation. Human engraftment was evaluated by flow cytometry of the injected right femur and non-injected bones and spleen. A threshold of 0.5% human $CD45^+$ cells in bone marrow was used as positive for human engraftment. Secondary transplantation was done by intrafemoral injection of cells from either right femur or pooled bone marrow from primary mice into one to three secondary mice pretreated with irradiation and antibody to CD122.

miRNA labeling

Target preparation was done according to (Lu et al., 2005). Briefly, two synthetic pre-labeled control nucleotides (5' – pCAGUCAGUCAGUCAGUCAGUCAG-3', and 5'-pGACCUCCAUGUAACGUACAA-3', Dharmacon) were spiked at 3fmoles per μg of total RNA to control for target preparation control. Small RNA's were recovered for 1-10 μg total RNA by PAGE purification and adaptor ligated sequentially on the 3' end and the 5' end using T4 RNA ligase (Amersham Biosciences). After reverse transcription using adaptor specific primers, products were PCR amplified for 18 cycles for 10 μg starting total RNA using 3' – primer 5'-TACTGGAATTCGCGGTTA-3' and 5' primer-biotin-CAAACGAATTCCTCACTAA-3'(IDT). PCR products were precipitated and dissolved in 66

μl TE buffer (10 mM Tris-HCL pH 8.0, 1 mM EDTA) containing two biotinylated post-labelling control oligonucleotides (100 fmoles of FVR506, 25 fmoles PTG20210).

Bead based detection

As described in (Lu et al., 2005), miRNA capture probes were conjugated to carboxylated xMAP beads (Luminex Corportion) in a 96-well plate. Samples were hybridized in a 96 well plate, with 2 mock PCR samples in each plate as a background control. Hybridization was carried out overnight. Beads were spun down, resuspended in 1x TMAC containing 10 $\mu g/mL^{-1}$ streptavividin-phycoerythrin (Molecular probes) before data acquisition of a Luminex 1001S machine. Median fluorescence intensity values were measured.

miRNA array computational analysis

Profiling data was scaled to the post-labelling controls and then the pre-labelling controls, in order to normalize readings from different probe/bead sets for the same sample and to normalize for the labelling efficiency, respectively. Data were threshholded at 32 and $\log_2$ transformed. The LSC miRNA signature was generated using a Smyth's moderated t-test with Benjamini-Hochberg multiple testing correction to compare fractions positive for LSCs versus those without LSCs.

Luciferase Reporter assay

Luciferase assay (Switchgear Genomics) was performed according to the manufacturers' protocol. Briefly, 293T cells were seeded to 40% confluency in 100 μl total volume in 96 well white TC plates (NUNC). The next day, equal volumes of mixture 1 (GoClone reporters; 30 ng/μl, miR-126 mimic or non-targeting mimic; 100 nM, and serum free media) was combined with mixture 2, (Dharmafect Duo/serum-free media) and incubated at room temperature RT for

20 minutes. After incubation, 4 volumes of pre-warmed serum-free media were added and mixed. 100 μl of the mixture was added to each well containing 293T cells and incubated overnight. Reconstituted luciferase substrate (100 μl) was added to each well, incubated at RT for 30 minutes and read for 2 seconds on a spectraMAX luminometer. Knockdown was determined by calculating the luciferase signal ratio for each reporter construct for miR-126 over the non-targeting control miRNA. GoClone control reporters used were GAPDH-3'UTR, ACTB-3'UTR, EMPTY-3'UTR, R01, and gene specific reporters were ADAM9-UTR, ILK-UTR, GOLPH3-3'UTR, CDK3-3'UTR and TOM1-3'UTR.

AML Stromal Chemotherapy Assay

Low passage MS5 stromal cells were seeded into 0.1% gelatin coated 96 well tissue culture plates and cultured for 48 hours in H5100 media (SCF; 100 ng/ml, TPO; 50 ng/ml. IL-7; 20 ng/ml, IL-3; 10 ng/ml, IL-6; 20 ng/ml, FLT3L; 10 ng/ml, G-CSF; 20 ng/ml, GM-CSF; 20 ng/ml) with 1% penicillin/streptomycin. After two days, primary patient AML cells (depleted for human T cells; $1x10^5$/well) were plated onto MS5 stroma and cultured overnight. After 24 hours, cells were treated with vehicle or with Daunorubicin/AraC (1:1 ratio; 50 ng/mL Daunorubicin and 500 ng/mL Ara-C) for 72 hours. Cells were recovered and evaluated for live cell content and immuno-phenotype by flow cytometry. Total RNA was recovered for qPCR detection of miR-126 levels.

Intracellular and Phosphoflow

Cultured 8227 cells were washed twice with 1x PBS and pelleted to eliminate culture medium. After washing, cells were stained for CD34 and CD38 cell surface antigens for 20 minutes at RT. Cells were washed and pelleted. Cells were immediately fixed with paraformaldehyde (final

concentration: 1.6%) for 10 minutes at room temperature. Cells were then centrifuged, washed once with PBS 1% BSA to remove residual PFA and permeabilized with ice-cold Perm buffer III (BD Phosflow for 30 min at 4°C followed by 2 washes in order to remove traces of methanol). Intracellular antibody staining was then performed. Phospho-Rb Ser807/811 was detected by a monoclonal antibody (clone D20B12; Cell Signaling), CDK3 was detected by a polyclonal antibody (clone D01P; Abnova) and detected by a donkey anti-rabbit brilliant violet 421 conjugated secondary antibody. Staining was performed by incubating permeabilized cells with the phospho-specific antibody for 30 minutes on ice and at dark, diluted in PBS 1% BSA at a final concentration of 1:50. After incubation, cells were washed in PBS 1% BSA and then stained in secondary antibody for 30 minutes at a final concentration of 1:50. Cells were analyzed by multi-parameter flow cytometry.

Western blot analysis

8227 cells were cultured as described and transduced with viral particles at a multiplicity of infection (MOI) of 30 for at least 16 hours. Cells were allowed to expand for 14 days and then flow sorted for mO^+ cells. Total cellular proteins were extracted with RIPA buffer (20 mM Tris-HCl (pH 7.4), 150 mM NaCl, 5 mM EDTA, 1% Triton X-100) supplemented with protease and phosphatase inhibitors: 1 mM PMSF, 10 mM NaF, 1 mM Na_3VO_4, CompleteMini™ and PhosStop ™ (Roche). Samples were resuspended in the lysis solution and incubated at 4°C for 30 minutes. Cell lysates were cleared by centrifugation at 10,000×g for 10 minutes at 4°C, and the supernatants were collected and assayed for protein concentration using Lowry assay based method (DC, BioRad). 40-50 micrograms of proteins were run on SDS-PAGE under reducing conditions. For immunoblotting, proteins were transferred to PVDF membranes, incubated with the specific antibody (anti-ADAM9 Cell Signaling #2099 1:1000, and ant-pan AKT Cell

Signaling # 4685 1:500, anti-PIK3R2 Cell Signaling #4257 1:1000, and GAPDH 1:10,000, Sigma) followed by peroxidase-conjugated secondary antibodies. Bands were visualized on Kodak BioMax film.

Lentiviral constructs, cell culture and colony formation

Lentiviral vector platforms for ectopic miRNA expression, stable knockdown and live cell miR-reporting were described previously (Gentner et al., 2010). Third generation lentiviral vector particles pseudotyped with VSV-G were generated as described (Guenechea et al., 2000).

8227 cell cultures were initiated from a primary patient sample with outgrowth after 1 month; this stock was used for all experiments. Primitive $CD34^+CD38^-$ 8227 cells were flow sorted and plated in culture media (described in Supplementary Experimental Procedures) for viral transduction and initiation of a new culture that re-establishes the cellular hierarchy. One to two weeks post viral transduction, cultures were re-sorted for $CD34^+CD38^-$ (LSC enriched), $CD34^+CD38^+$ (leukemia progenitor enriched) and $CD34^-CD38^+$ (mature AML blasts) populations for experimental culture studies or colony assays. Individual cultures were passaged weekly and monitored with phenotypic cell surface markers.

For chemotherapy experiments, $1x10^5$ transduced 8227 cells were plated into 96-well plates, exposed the following day to a dose range of Daunorubincin and analyzed using CD34 and CD38 cell surface markers 72 hours later. $CD34^+$ levels were normalized to vehicle only wells.

Ki67 and Hoechst flow cytometry

Cells were stained for surface markers, washed and fixed using BD Cytofix buffer, washed and permeabilized with BD Perm 2 (BD), washed and stained with PE- or FITC- or PerCP-Cy5.5

conjugated Ki67 antibody (BD) and finally resuspended in BD Cytofix buffer with Hoechst at 1 μg/mL. The cells were then analyzed on a BD LSRII machine with a UV laser.

Quantitative PCR

miR-126 expression was analyzed as described (Lechman et al., 2012). Briefly, small RNAs were extracted using Trizol (Life Technologies) and miRNA expression levels were determined by the Applied Biosystems Taqman® microRNA Assay system. Reactions were carried out in triplicate in an ABI Prism 7900HT (Applied Biosystems, Foster City, CA). miRNA expression was normalized to RNU48.

Statistical analysis

Unless otherwise indicated, mean $\pm$ SEM values are reported in the graphs. For pairwise comparisons, a Mann-Whitney non-parametric test was used unless otherwise indicated.

SUPPLEMENTAL REFERENCES

Borgan, Ø. (2001). Modeling Survival Data: Extending the Cox Model. Terry M. Therneau and Patricia M. Grambsch, Springer-Verlag, New York, 2000. No. of pages: xiii + 350. Price: $69.95. ISBN 0-387-98784-3. Stat. Med. *20*, 2053–2054.

Cheson, B.D., Bennett, J.M., Kopecky, K.J., Büchner, T., Willman, C.L., Estey, E.H., Schiffer, C.A., Doehner, H., Tallman, M.S., Lister, T.A., et al. (2003). Revised recommendations of the International Working Group for Diagnosis, Standardization of Response Criteria, Treatment Outcomes, and Reporting Standards for Therapeutic Trials in Acute Myeloid Leukemia. J. Clin. Oncol. Off. J. Am. Soc. Clin. Oncol. *21*, 4642–4649.

Cox, J., and Mann, M. (2008). MaxQuant enables high peptide identification rates, individualized p.p.b.-range mass accuracies and proteome-wide protein quantification. Nat. Biotechnol. *26*, 1367–1372.

Fei, D.L., Koestler, D.C., Li, Z., Giambelli, C., Sanchez-Mejias, A., Gosse, J.A., Marsit, C.J., Karagas, M.R., and Robbins, D.J. (2013). Association between In Utero arsenic exposure, placental gene expression, and infant birth weight: a US birth cohort study. Environ. Health Glob. Access Sci. Source *12*, 58.

Geiss, G.K., Bumgarner, R.E., Birditt, B., Dahl, T., Dowidar, N., Dunaway, D.L., Fell, H.P., Ferree, S., George, R.D., Grogan, T., et al. (2008). Direct multiplexed measurement of gene expression with color-coded probe pairs. Nat. Biotechnol. *26*, 317–325.

Guenechea, G., Gan, O.I., Inamitsu, T., Dorrell, C., Pereira, D.S., Kelly, M., Naldini, L., and Dick, J.E. (2000). Transduction of human CD34+ CD38- bone marrow and cord blood-derived SCID-repopulating cells with third-generation lentiviral vectors. Mol. Ther. J. Am. Soc. Gene Ther. *1*, 566–573.

Hermjakob, H., and Apweiler, R. (2006). The Proteomics Identifications Database (PRIDE) and the ProteomExchange Consortium: making proteomics data accessible. Expert Rev. Proteomics *3*, 1–3.

Hu, Y., and Smyth, G.K. (2009). ELDA: extreme limiting dilution analysis for comparing depleted and enriched populations in stem cell and other assays. J. Immunol. Methods *347*, 70–78.

Johnson, W.E., Li, C., and Rabinovic, A. (2007). Adjusting batch effects in microarray expression data using empirical Bayes methods. Biostat. Oxf. Engl. *8*, 118–127.

Kulak, N.A., Pichler, G., Paron, I., Nagaraj, N., and Mann, M. (2014). Minimal, encapsulated proteomic-sample processing applied to copy-number estimation in eukaryotic cells. Nat. Methods *11*, 319–324.

Lu, J., Getz, G., Miska, E.A., Alvarez-Saavedra, E., Lamb, J., Peck, D., Sweet-Cordero, A., Ebert, B.L., Mak, R.H., Ferrando, A.A., et al. (2005). MicroRNA expression profiles classify human cancers. Nature *435*, 834–838.

Merico, D., Isserlin, R., Stueker, O., Emili, A., and Bader, G.D. (2010). Enrichment map: a network-based method for gene-set enrichment visualization and interpretation. PloS One *5*, e13984.

Reimand, J., Arak, T., and Vilo, J. (2011). g:Profiler--a web server for functional interpretation of gene lists (2011 update). Nucleic Acids Res. *39*, W307–W315.

Rudy, J., and Valafar, F. (2011). Empirical comparison of cross-platform normalization methods for gene expression data. BMC Bioinformatics *12*, 467.

Sirinukunwattana, K., Savage, R.S., Bari, M.F., Snead, D.R.J., and Rajpoot, N.M. (2013). Bayesian hierarchical clustering for studying cancer gene expression data with unknown statistics. PloS One *8*, e75748.

Smoot, M.E., Ono, K., Ruscheinski, J., Wang, P.-L., and Ideker, T. (2011). Cytoscape 2.8: new features for data integration and network visualization. Bioinforma. Oxf. Engl. *27*, 431–432.

Subramanian, A., Tamayo, P., Mootha, V.K., Mukherjee, S., Ebert, B.L., Gillette, M.A., Paulovich, A., Pomeroy, S.L., Golub, T.R., Lander, E.S., et al. (2005). Gene set enrichment analysis: a knowledge-based approach for interpreting genome-wide expression profiles. Proc. Natl. Acad. Sci. U. S. A. *102*, 15545–15550.